Perturbation Study on the Reaction of C_2 with N_2 in High-Temperature C_{60}/Ar + N_2 Mixtures

T. Sommer, T. Kruse, and P. Roth*

Institut für Verbrennung und Gasdynamik, Gerhard-Mercator-Universität Duisburg, D-47048 Duisburg, Germany

H. Hippler

Institut für Physikalische Chemie, Universität Karlsruhe, D-76128 Karlsruhe, Germany

Received: September 10, 1996; In Final Form: December 29, 1996[⊗]

The reaction of C_2 radicals with nitrogen was studied behind reflected shock waves by time dependent absorption and emission measurements. Mixtures of fullerene C_{60} highly diluted in argon were shock heated and used as C_2 sources. Perturbation of the reaction system by addition of N_2 results in changes of C_2 absorption and causes strong CN emission. The C_2 concentration was quantitatively monitored by ring dye laser absorption spectroscopy at $\nu = 19\,355.60$ cm^{-1}. Simultaneously, the time behavior of spectrally resolved light emitted from the shock-heated mixtures was recorded by an intensified CCD camera in the wavelength range 315 nm $\leq \lambda \leq$ 570 nm. By comparing the integrated C_2 and CN emission signals for the $\Delta v = 0$ progressions, the CN concentration can be determined on the basis of the known C_2 concentration and the relative line strengths. The experiments were performed in the temperature range 2896 K $\leq T \leq$ 3420 K at pressures 1.68 bar $\leq p \leq$ 2.03 bar. Evaluation of C_2 and CN concentration measurements lead to the following rate coefficient for the reaction $C_2 + N_2 \rightleftharpoons CN + CN$: k_3 1.5×10^{13} exp(−21 000 K/T) cm^3 mol^{-1} s^{-1}. The uncertainty in k_3 is expected to be ±50%.

Introduction

High-temperature reactions of C atoms and C_2 radicals with nitrogen are of great importance in the combustion chemistry of hydrocarbons. Kinetic models describing NO formation in the primary reaction zone of combustion waves consider radicals like C, C_2, and CH to break the N≡N bond, thus enabling the intermediate species to participate in subsequent reaction steps. Fenimore[1] suggested that prompt NO formation in hydrocarbon flames might be initiated by the reactions

$$CH + N_2 \rightleftharpoons HCN + N$$

$$C_2 + N_2 \rightleftharpoons CN + CN \qquad \text{(R3)}$$

followed by the oxidation of the products to form NO. Other studies try to explain the rapid NO formation by reactions of other hydrocarbon radicals with N_2. The backward direction of (R3) has been investigated in two shock tube studies. Patterson and Greene[2] monitored CN and C_2 emission during the pyrolysis of 1−5% BrCN diluted in argon. Fairbairn[3] observed the decay in CN concentration after thermal decomposition of C_2 N_2. Rate coefficients obtained from these works differ by a factor of more than 150 in the preexponential factor and more than a factor of 2 in the activation energy. On the basis of these studies, Baulch et al.[4] recommend a value of $k_{-3} = 1 \times 10^{13}$ cm^3 mol^{-1} s^{-1} at 4500 K, but the great difference in activation energy prevents any evaluation of temperature dependence.

The aim of the present work was to study reaction R3 by monitoring both C_2 and CN in high-temperature experiments. The pyrolysis of fullerene C_{60} was used as a well-characterized C_2 source perturbated by addition of N_2 concentrations between 0.4% and 5.2%. Two different diagnostic tools were applied to follow the shock-induced reaction of C_2 with N_2. A ring dye laser spectrometer was used to detect the time dependent C_2 formation by absorption measurements in the (0−0) band of the $d^3\Pi_g \leftarrow a^3\Pi_u$ transition of C_2. Simultaneously, the light emitted by the shock-heated C_{60}/N_2/Ar mixture was spectrally and time dependently resolved and recorded by an intensified CCD camera in the wavelength range 315 nm $\leq \lambda \leq$ 570 nm.

Experimental Section

The experimental setup used during the present study is schematically shown in Figure 1. It consists of an aerosol generator for dispersing the fullerene powder, the main shock tube for heating the C_{60} containing mixtures to high temperatures, a ring dye laser spectrometer for measuring C_2 absorption, a spectrograph with intensified CCD camera for the detection of spectral and time-resolved emission, and an IR diode laser system.

The C_{60} powder was dispersed in argon by an expansion wave driven aerosol generator.[5] It consists of a glass vessel of $V = 3 \times 10^4$ cm^3 volume connected to a glass tube of 5 cm inner diameter, which was separated by a thin diaphragm from a high-pressure tube of the same diameter. A thin dispersion plate was positioned near the diaphragm, which carried for every experiment about 100 mg of the fullerene powder. Before the powder dispersion was started, the low-pressure section of the aerosol generator was evacuated to a pressure of about 5×10^{-5} mbar. Subsequently, argon was filled into the high-pressure tube. After the bursting of the diaphragm, the high-pressure gas argon expanded in the form of a supersonic expansion wave into the evacuated vessel, thus dispersing the fullerene powder and bringing it into aerosol form. The fullerene C_{60} powder used during the present experiments was supplied by Hoechst AG, Germany, with a purity better than 99.7%. The generated aerosol was mixed with N_2/Ar mixtures and subsequently filled into the running section of the main shock tube.

* Author to whom correspondence should be addressed.
⊗ Abstract published in *Advance ACS Abstracts,* May 1, 1997.

S1089-5639(96)02779-X CCC: $14.00

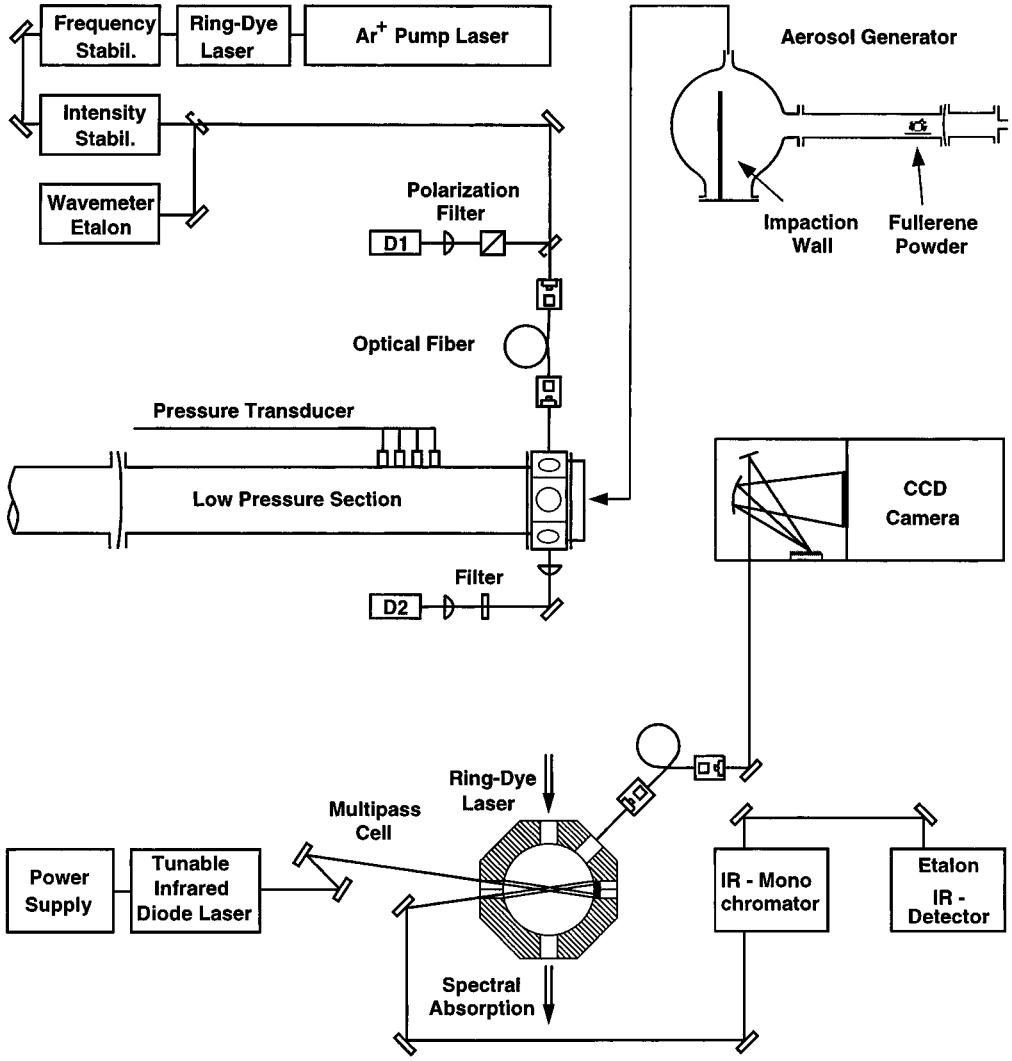

Figure 1. Schematic of the experimental setup including shock tube, aerosol generator, and different optical diagnostics.

The stainless steel shock tube, which was used as an isothermal−isobaric reactor, has an inner diameter of 8 cm, a total length of 11 m, and a running section of 7.2 m in length. The initial pressure of the aerosol measured by calibrated diaphragm type pressure transducers was in the range from 19 to 30 mbar. The shock velocity was measured by piezoelectric pressure transducers positioned at known distances along the shock tube axis. The postshock temperature and pressure were calculated from the incident shock speed by applying one-dimensional conservation equations. The shock wave running into the fullerene-containing aerosol caused a sudden temperature and pressure increase initiating first the evaporation of the solid fullerene particles in less than 3 μs. Subsequently, the fullerene vapor started to decompose; see also refs 6 and 7.

The optical setup for measuring time dependent C_2 absorption consists of a ring dye laser spectrometer (Spectra-Physics RDL 380 D), which was connected to the measurement section of the main shock tube by an optical fiber. The laser light passing through the shock tube was spectrally absorbed, and the resulting time dependent C_2 absorption during the high-temperature reaction was determined with a fast Si detector. A second Si detector was used to record the incident laser light intensity. The laser was fixed to the line center wavenumber at $\nu = 19355.60$ cm^{-1} corresponding to an overlap of nine rotational lines in the (0−0) band head of the $d^3\Pi_g \leftarrow a^3\Pi_u$ transition of C_2. Due to uncertainties in the exact position of these rotational lines,[8,9] additional shock tube experiments were performed with mixtures of acetylene as well as fullerene C_{60}, in each case highly diluted in argon. The comparison of C_2 absorption signals during the pyrolysis of both C_2H_2 and C_{60} measured earlier in the (1−0) band at $\nu = 21\,393.12$ cm^{-1} [7,10] and the absorption signals in the (0−0) band head at $\nu = 19\,355.60$ cm^{-1} during the present study made it possible to determine the line shape of the overlap of the selected absorption lines. For the determination of absolute C_2 concentration, spectroscopic data obtained from radiative lifetime measurements[11] were used. The respective oscillator strength of the C_2 swan system is within about 15% in agreement with our own oscillator strength measurement in the (0−0) band head of C_2. Our value of $f_{00} = 0.037 \pm 0.002$ was obtained from shock tube pyrolysis of C_2H_2; see ref 10. So, absorption signals measured in the (0−0) band head were calibrated with calculated and measured absorption in the (1−0) band. Additional shock tube experiments in $C_{60}/N_2/Ar$ mixtures were conducted, and spectral absorption at $\nu = 19\,354.00$ cm^{-1} was measured. This allows the determination of the interference absorption of the (0−3) band head of the $B^2\Sigma^+ \leftarrow X^2\Sigma^+$ transition of CN. The absorption profiles were stored in a transient recorder and transmitted to a personal computer for further data processing. To achieve a low detection limit, it was necessary to stabilize both the frequency and the intensity of the dye laser. A complete despription of technical details of the spectrometer is given in ref 12.

The light emitted from the shock-heated reactive gas mixture

was focused via a light fiber at the entrance slit of a $^1/_8$ m spectrograph, which has a spectral range of $\Delta\lambda = 255$ nm and a resolution of 1.3 nm. The spectrally resolved light was detected by an intensified CCD camera allowing a fast time shift of the optical information. For this purpose only a few lines at the top of the CCD sensor chip were illuminated for a certain time interval. The stored spectral emission was stepwise transferred line by line into the dark zone of the CCD chip, which served as a memory. In this way, the spectral as well as the temporal behavior of the emitted light could be recorded. Spectral characteristics of the quantum efficiency of the intensifier and of the diffraction grid were taken into account. The intensified CCD camera system (Streak Star) with spectrograph was supplied by L.A. Vision.

For a quantitative data interpretation in terms of kinetic parameters, the initial concentration of C_{60} was required. For this purpose fullerene C_{60} powder was dispersed in Ar containing about 6% of O_2. The aerosol mixtures were heated by the shock wave to conditions similar to the experiments of the present study and resulted in a complete oxidation of C_{60} by O_2. The gas phase oxidation products CO and CO_2 were quantitatively measured by tunable infrared diode laser spectroscopy, from which an initial C_{60} gas phase concentration of about 40 ppm could be deduced.

Results

The experiments on high-temperature $C_{60}/N_2/Ar$ mixtures were conducted behind reflected shock waves at temperatures between 2896 and 3420 K and at pressures between 1.68 and 2.03 bar. In 13 individual experiments conducted in $C_{60}/N_2/Ar$ mixtures with N_2 concentrations ranging between 0.4% and 5.2%, the C_2 absorption signals at $\nu = 19\,355.60$ cm^{-1} and the spectrally resolved emission signals were recorded. To quantify possible interference absorption of CN, a second group of experiments was performed under similar conditions at $\nu = 19\,354.00$ cm^{-1}. This wavenumber has been selected to study interference absorption of CN for two reasons. On the one hand ring dye laser absorption spectroscopy measurements at $\nu = 19\,354.00$ cm^{-1} performed during the pyrolysis of fullerene in C_{60}/Ar mixtures at high temperatures showed no spectral absorption of C_2. On the other hand the time behavior of CN emission signals recorded in $C_{60}/N_2/Ar$ mixtures was in excellent agreement with the interference absorption measurements. We therefore can assume that measured interference signals at $\nu = 19\,354.00$ cm^{-1} are related to absorption in the (0−3) band head of the $B^2\Sigma^+ \leftarrow X^2\Sigma^+$ transition of CN.

Typical examples of C_2 absorption profiles obtained from shock-heated fullerene/argon-mixtures without and with addition of N_2 are shown in Figure 2 together with the interference absorption for nearly the same experimental conditions. The C_2 profile measured in the experiment without N_2 shows a fast increase and a characteristic decrease after reaching maximum absorption followed by a steady state behavior for the rest of the observation time. This illustrates together with a detailed kinetic interpretation that the pyrolysis of fullerene C_{60} can serve as a well-known C_2 source; see also ref 7. The addition of N_2 results in a strong decrease of the measured C_2 radical concentration after rapid formation. This principle behavior was found in all experiments. Each individual absorption profile obtained from shock-heated $C_{60}/N_2/Ar$ mixtures was converted to C_2 concentration via Lambert−Beer's law taking the interference CN absorption into account. The experimental conditions and characteristics of measured C_2 concentration profiles are summarized in Table 1.

The combination of measured C_2 concentration and measured spectrally resolved C_2 and CN emission recorded with the CCD camera permits the evaluation of the CN emission in terms of CN concentration profiles. For this purpose the emission signals $\epsilon(\lambda)$ of the $\Delta v = 0$ progressions of C_2 and CN were integrated with respect to the wavelength at a fixed time τ for each individual experiment. In this way integrated emission signals $I_{C_2}^{(\tau)}$ and $I_{CN}^{(\tau)}$ for C_2 and CN at a fixed time τ were defined by

$$I_{C_2}^{(\tau)} = \int_{490\text{ nm}}^{522\text{ nm}} \epsilon(\lambda)\,\mathrm{d}\lambda \qquad I_{CN}^{(\tau)} = \int_{377\text{ nm}}^{392\text{ nm}} \epsilon(\lambda)\,\mathrm{d}\lambda$$

A typical example of spectrally resolved emission for one shock tube experiment at $\tau = 150$ μs after shock arrival is shown in Figure 3. Oscillator strengths f_{i-i,C_2} and $f_{i-i,CN}$ for vibrational bands ($i = 0-3$) of the two radical species, which significantly contribute to the emission for our conditions are reported in the literature.[8,9,13,14] The knowledge of the absolute C_2 concentration $[C_2]^{(\tau)}$ at time τ from ring dye laser absorption measurements enables calibration of the CN concentration at time τ, $[CN]^{(\tau)}$, by

$$\frac{I_{CN}^{(\tau)}}{I_{C_2}^{(\tau)}} = \frac{[CN]^{(\tau)}}{[C_2]^{(\tau)}} \sum_i \frac{f_{i-i,CN}}{f_{i-i,C_2}} \frac{\nu_{CN}^3 \exp(-hc\nu_{CN}/kT)}{\nu 2_C^3 \exp(-hc\nu_{C_2}/kT)} \qquad (1)$$

The properties ν_{CN} and ν_{C_2} are the respective mean band wavenumbers of CN and C_2. After calibration of the CN emission against CN concentration at one fixed time τ via C_2 concentration, the proportionality factor between emission and concentration of CN is known for the whole time scale of this specific shock tube experiment. This calibration procedure was repeated for each individual shock tube experiment to evaluate the measured CN emission in terms of CN concentration for the whole reaction time. All experimental results obtained are also summarized in terms of CN concentrations in Table 1.

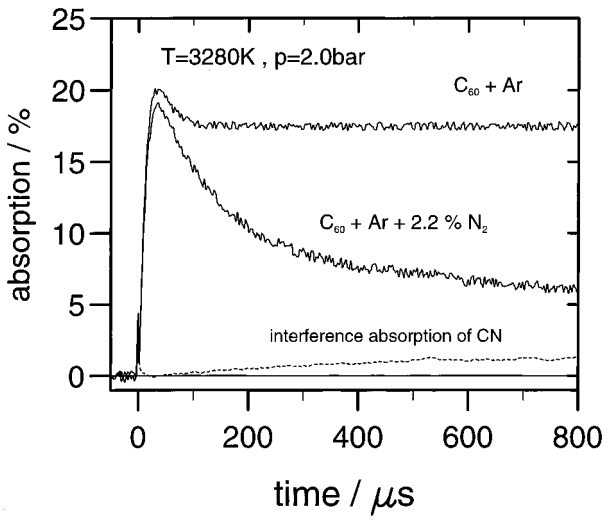

Figure 2. Examples of time dependent C_2 absorption measured in C_{60}/Ar and $C_{60}/N_2/Ar$ mixtures.

Discussion

It can be assumed that several subsequent processes occur in the shock-heated gases containing C_{60} in highly dispersed particle form. Due to the relatively high vapor pressure of C_{60} the solid agglomerated carbonaceous particles evaporate rapidly at high temperatures. This process starts behind the incident shock wave, where temperatures are in the range 1200 K $\leq T \leq$ 1600 K, and continues behind the reflected wave much more rapidly because of the higher temperature level. The particle size after powder dispersion was determined by scanning

TABLE 1: Experimental Conditions and C_2 and CN Concentration Characteristics Obtained in High-Temperature $C_{60}/N_2/Ar$ Reaction Systems[a]

T/K	*p*/bar	% N_2	$t([C_2]_{max})/\mu s$	$[C_2]_{max}$	$[C_2]_{100\,\mu s}$ $[CN]_{100\,\mu s}$	$[C_2]_{300\,\mu s}$ $[CN]_{300\,\mu s}$	$[C_2]_{500\,\mu s}$ $[CN]_{500\,\mu s}$	$[C_2]_{700\,\mu s}$ $[CN]_{700\,\mu s}$
2896	1.90	3.22	162	2.02	1.73	1.87	1.64	1.44
					1.23	4.21	7.02	10.53
2983	2.02	2.69	110	3.33	3.27	2.53	2.00	1.67
					1.54	8.08	14.04	18.85
3022	2.14	4.98	114	3.33	3.30	2.15	1.53	1.21
					4.07	15.93	23.33	28.90
3120	1.92	1.93	75	4.38	4.21	3.03	2.19	1.77
					2.55	8.80	14.12	18.06
3123	2.01	0.45	69	4.43	4.22	3.91	3.57	3.35
					0.64	3.46	6.67	9.23
3178	1.93	3.33	47	4.90	3.95	1.90	1.38	1.14
					5.88	17.06	21.76	25.59
3178	2.01	3.33	47	4.51	3.53	1.96	1.27	1.08
					5.36	16.88	22.23	25.71
3183	2.11	5.15	45	5.32	4.16	1.26	0.79	0.63
					7.81	20.31	24.48	27.08
3280	2.00	2.20	32	5.26	3.95	2.11	1,58	1.26
					4.76	14.52	19.76	22.62
3343	2.07	5.15	29	6.97	3.19	1.11	0.90	0.69
					12.62	22.71	26.36	29.44
3400	1.84	5.15	25	5.96	2.42	0.91	0.67	0.55
					11.39	19.17	22.78	24.17
3408	2.03	1.98	23	7.56	3.71	2.04	1.60	1.31
					7.84	16.91	20.60	23.28
3420	1.68	5.15	22	6.30	2.34	0.84	0.66	0.52
					9.15	16.52	18.75	21.88

[a] All concentrations in 10^{13} cm^{-3}.

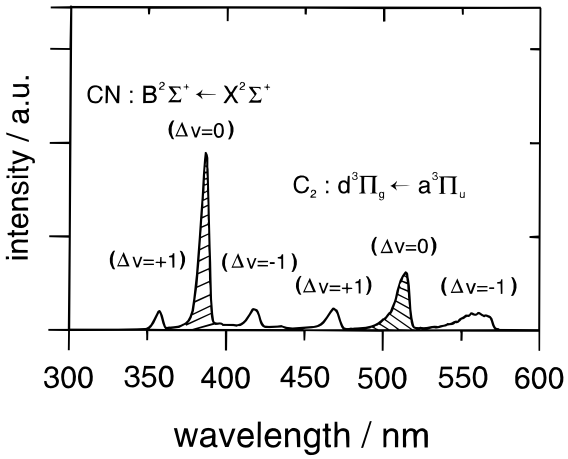

Figure 3. Example of the spectral emission of shock-heated $C_{60}/N_2/Ar$ mixtures at $\tau = 150$ μs after shock arrival.

electron microscopy resulting in particle diameters of less than 900 nm. An upper limit for a fullerene particle evaporation time of about 3 μs can be calculated[6] for conditions of the present study. The given upper limit for the evaporation time was experimentally confirmed by laser light-scattering experiments behind shock waves.[6] We therefore can assume for our experimental conditions that the initial reactant C_{60} is in the vapor phase for nearly the complete observation time and that reactions described in this study are dominated by homogeneous gas phase kinetics.

A shock tube study on the pyrolysis of fullerene C_{60} reported earlier[7] revealed that C_2 formation measured in C_{60}/Ar mixtures at high temperatures can be described by two reactions: a direct C_2 abstraction from the fullerene structure initiating the thermal decomposition of C_{60} (R1) and a removal of the C_2 concentration by a bimolecular $C_2 + C_2$ reaction (R2).[7,10]

$$C_{60} \rightarrow C_2 + C_{58} \qquad \text{(R1)}$$

$$C_2 + C_2 \rightleftharpoons C_3 + C \qquad \text{(R2)}$$

Two different models[7] for the further breakdown of fullerene fragments have been discussed in detail, which are not of importance here. The rate coefficient for the reverse direction of (R2), k_{-2}, was calculated on the basis of the equilibrium constant with a modified value for the heat of formation of C_2, which was slightly reduced by about 3% from the JANAF data.[15] This variation of the thermodynamic data was confirmed by recent measurements in different reaction systems.[7,10,16] The above two reactions together with the respective rate coefficients were found to be sufficient to characterize our C_2 source for all experimental conditions studied.

It seems reasonable to interpret the strong change in C_2 concentration caused by the addition of N_2 (see Figure 2) by a direct reaction between these species:

$$C_2 + N_2 \rightleftharpoons CN + CN \qquad \text{(R3)}$$

Reaction R3 allows the description of both experimental observations, the decrease in C_2 concentration and also the formation of CN. Secondary reactions of the products of (R2) and (R3) can also contribute to the time evolution of C_2 and CN. Most important in the present case is the reaction of C atoms with N_2:

$$C + N_2 \rightleftharpoons CN + N \qquad \text{(R4)}$$

The rate coefficient was determined by Dean et al.[17] and Lindackers et al.[18] during perturbation studies in $C_2H_6/N_2/Ar$ and $CH_4/N_2/Ar$ reaction systems. Both values are in excellent agreement; they differ by less than 10% in the temperature range 2900 K $\leq T \leq$ 3400 K. This value was recently confirmed by Natarajan et al.[19] It is obvious that (R4) also affects the C_2 concentration via the reverse direction of the quasi-equilibrated reaction R2. A rate expression for k_4 used for calculations during the present study is given in Table 2. A further important secondary reaction, which influences both the C_2 and CN

TABLE 2: Simplified High-Temperature Reaction Mechanism of the C_{60}/N_2 System Highly Diluted in Ar[a]

	reaction	A[b]	B/K	ref
(R1)	$C_{60} \rightarrow C2 + C_{58}$	4.0×10^{12}	61 940	7
(R2)	$C_2 + C_2 \rightleftharpoons C + C_3$	2.0×10^{15}	9 020	7, 10
(R3)	$C_2 + N_2 \rightleftharpoons CN + CN$	1.5×10^{13}	21 000	this study
(R4)	$C + N_2 \rightleftharpoons CN + N$	4.5×10^{13}	22 000	18
(R5)	$C + CN \rightleftharpoons C_2 + N$	3.0×10^{14}	18 120	21

[a] $k_i = A \cdot \exp(-B/T)$. Backward rate coefficients calculated on the basis of JANAF thermodynamic data with slightly reduced heat of formation for C_2 (see text). [b] Units for (R1) are s^{-1}; units for (R2)−(R5) are $cm^3\ mol^{-1}\ s^{-1}$.

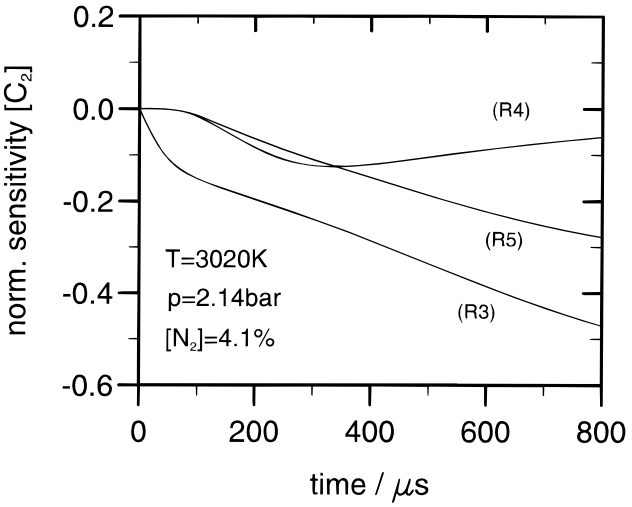

Figure 4. Normalized sensitivity coefficients (see text) of reactions R3−R5 describing the influence on C_2 concentration.

concentration, is

$$C + CN \rightleftharpoons C_2 + N \qquad \text{(R5)}$$

A rate coefficient for this reaction given by Slack and Fishburne[4,20] was later revised by Slack,[21] see Table 2. The complete reaction mechanism used for evaluating the present experiments is summarized in Table 2 together with rate coefficients reported in the literature.

A detailed sensitivity analysis of the above mechanism was done using the SENKIN program code[22] to study the contribution of the different elementary reactions of Table 2 to the computed C_2 and CN profiles. With the normalized sensitivity coefficients defined in the usual way by

$$S_{X,i} = \frac{k_i\ \partial[X]}{[X]\ \partial k_i}$$

the influence of variations of the different rate coefficients on the measured properties was analyzed. Figures 4 and 5 show examples of the sensitivity coefficients for reactions R3−R5 with respect to C_2 and CN as a function of time. The reaction conditions chosen were typical for the present perturbation experiments. In each case, the strongest influence on both C_2 and CN concentrations is clearly correlated to (R3), which dominates the sensitivity analysis for the whole reaction time scale of 800 μs. Reactions R4 and R5 involving the secondary reactions of C are less sensitive and have a minor influence. Similar results were calculated for all experiments performed during the present study. This sensitivity calculation clearly underlines that the main contribution to the decrease of C_2 and the formation of CN is related to reaction R3.

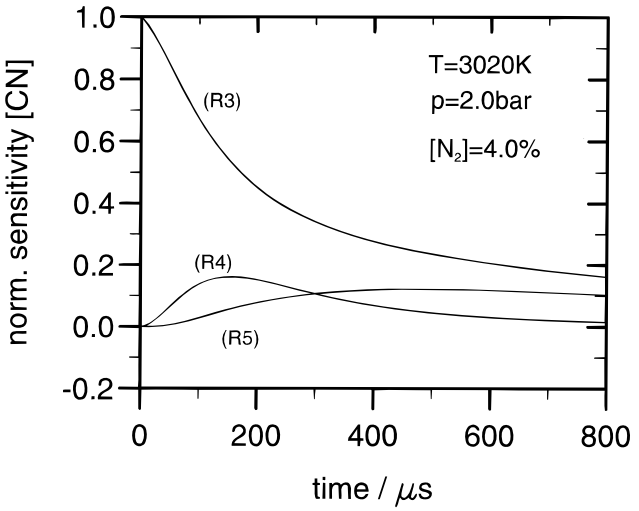

Figure 5. Normalized sensitivity coefficients (see text) of reactions R3−R5 describing the influence on CN concentration.

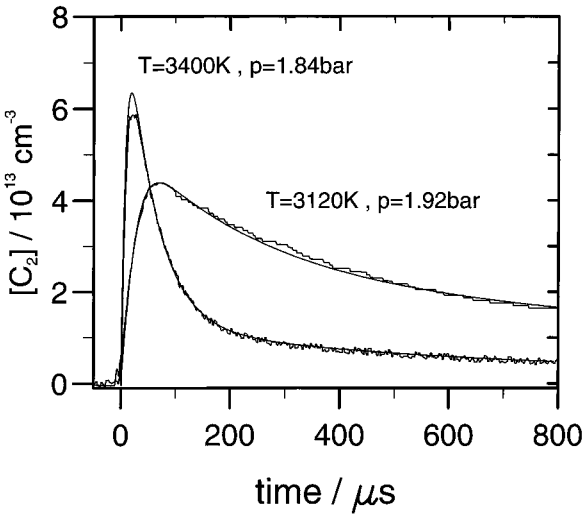

Figure 6. Comparison between measured (noisy lines) and calculated (solid lines) C_2 concentration profiles for two different temperatures.

The strategy for evaluating the measured C_2 and CN profiles in terms of a rate coefficient k_3 seems to be clear from the above analysis. For each individual shock tube experiment, measured concentrations were compared with computer simulations based on the mechanism of Table 2 with rate coefficient k_3 being a variable parameter to achieve a good fitting of both C_2 and CN profiles. Examples obtained from two different shock tube experiments are illustrated in Figure 6 for C_2 and in Figure 7 for CN. The resulting rate coefficients k_3 used as best fit parameters were identical for adapting C_2 and CN. Nearly complete agreement between calculated and measured concentration profiles for the two examples in Figures 6 and 7 as well as for all other experiments was obtained, although only a rather simple mechanism was used to explain the experimental findings. The results indicate that further reactions of expected fullerene fragments and other intermediate species should have only a minor influence on the measured properties. The mechanism of Table 2 seems to be sufficient to describe both the time dependent C_2 source and the perturbation by N_2. The individual rate coefficients k_3 obtained as best fit parameters are summarized in the Arrhenius diagram of Figure 8. The data points are well approximated by the solid line which can be expressed by:

$$k_3 = 1.5 \times 10^{13} \exp(-21\,000\ \text{K}/T)\ \text{cm}^3\ \text{mol}^{-1}\ \text{s}^{-1}$$

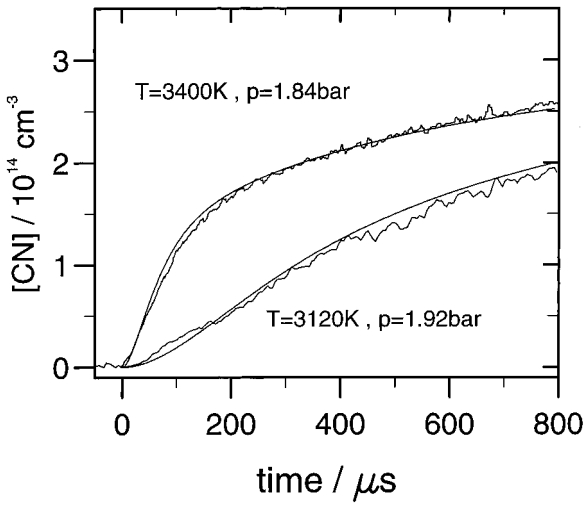

Figure 7. Comparison between measured (noisy lines) and calculated (solid lines) CN concentration profiles for two different temperatures.

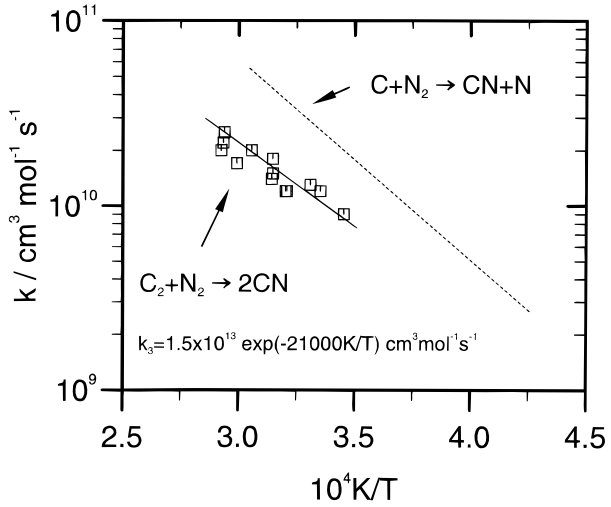

Figure 8. Arrhenius diagram for rate coefficient k_3 determined in the present study compared with rate coefficient k_4 reported earlier.[18]

The scattering of the data points around the given mean value is comparatively low. The activation energy is similar to the value determined by Patterson and Greene[2] calculated from the reverse reaction, while the activation energy given by Fairbairn[3] is much higher. The absolute magnitude of rate coefficient k_3 determined in the present study is below the values reported in the literature,[2,3] which perhaps could be explained by the fact that both earlier works did not consider any C_2 and CN-removing side reactions, although the experiments were performed in mixtures with relatively high reactant concentrations. The dotted line in Figure 8 illustrates the rate coefficient k_4 determined by Lindackers et al.[18] A comparison between k_3 and k_4 extrapolated to moderate combustion temperatures around 2000 K shows that both C and C_2 might break the strong N≡N bond with similar efficiency. As a consequence, reactions R3 and R4 should both be considered for the prompt NO formation in hydrocarbon flames.

Conclusion

Mixtures of fullerene C_{60} highly diluted in argon were shock heated and used as well-characterizable thermal C_2 sources. A simplified kinetic model developed earlier is able to predict the C_2 concentration. The reaction system was perturbed by addition of N_2 resulting in changes of the C_2 concentration and in the formation of CN. C_2 was measured by ring dye laser absorption spectroscopy, while both C_2 and CN emission were recorded by an intensified CCD camera. A comparison of the integrated C_2 and CN emission together with C_2 absorption measurements was used to evaluate the CN concentration. A kinetic model was developed to describe the time behavior of the measured molecular species. The reaction $C_2 + N_2 \rightleftharpoons CN + CN$ was most sensitive to measured properties, and its rate coefficient could be determined.

Acknowledgment. This work is originated in the Sonderforschungsbereich 209 of the Universität Duisburg. The financial support of the Deutsche Forschungsgemeinschaft is gratefully acknowledged.

References and Notes

(1) Fenimore, C. P. Formation of nitric oxide in premixed hydrocarbon flames. *Thirteenth Symosium (International) on Combustion*; The Combustion Institute; 1971; pp 373−380.

(2) Patterson, W. L.; Greene, E. F. Kinetic Study of the Formation and Reaction of CN Molecules in Shock Waves. *J. Chem. Phys.* **1962**, *36* (5), 1146−1151.

(3) Fairbairn, A. R. Temperature measurements of C_2 and CN radicals generated in a shock tube. I. Pyrolysis in the absence of oxygen. *Proc. R. Soc. London* **1961**, *A267*, 88−101.

(4) Baulch, D. L.; Duxbury, J.; Grant, S. J.; Montague, D. C. *Evaluated kinetic data for high temperature reactions*; American Chemical Society: Washington, DC, 1981; Vol. 10.

(5) Rajathurai, A. M.; Roth, P.; Fissan, H. A Shock and Expansion Wave-driven Powder Disperser. *Aerosol Sci. Technol.* **1990**, *12*, 613−619.

(6) von Gersum, S.; Kruse, T.; Roth, P. Spectral Emission During High Temperature Pyrolysis of Fullerene C_{60} in Shock Waves. *Ber. Bunsen-Ges. Phys. Chem.* **1994**, *98*, 979−982.

(7) Sommer, T.; Kruse, T.; Roth, P. C_2 formation during high-temperature pyrolysis of fullerene C_{60} in shock waves. *J. Phys. Chem.* **1995**, *99* (36), 13509−13512.

(8) Phillips, J. G.; Davis, S. P. *The Swan System of the C2 Molecule*; University of California Press: Berkeley, CA, 1968.

(9) Danylewych, L. L.; Nicholls, R. W. Intensity measurements on the C_2 ($d^3\Pi_g - a^3\Pi_u$) swan band system I. Intercept and partial band methods. *Proc. R. Soc. London A.* **1974**, *339*, 197−212.

(10) Kruse, T.; Roth, P. Kinetics of C_2-Radical Reactions During Shock-induced Pyrolysis of Acetylene. *J. Chem. Phys.*, in press.

(11) Naulin, C.; Costes, M.; Dorthe, G. C_2 Radicals in a supersonic molecular beam. Radiative livetime of the $d^3\Pi_g$ state measured by laser-induced fluorescene. *Chem. Phys. Lett.* **1988**, *5* (143), 496−500.

(12) Markus, M. W.; Roth, P. On the Reaction of CH with CO Studied in High Temperature CH_4/Ar Mixtures. *Int. J. Chem. Kinet.* **1992**, *24*, 433−445.

(13) Lavendy, H.; Gandara, G.; Robbe, J. M. Oscillator strengths, radiative lifetimes, and photodissociation cross-sections for CN. *J. Mol. Spectrosc.* **1984**, *106*, 395−410.

(14) Colket, M. B. Spectroscopic absorption model for CN($X^2\Sigma \rightarrow B^2\Sigma$): Comparison of experiments and theory. *J. Quant. Spectrosc. Radiat. Transfer* **1984**, *31* (1), 7−13.

(15) Chase, M. W.; Davies, C. A.; Downey, J. R.; Frurip, D. J.; McDonald, R. A.; Syverud, A. N. *JANAF Thermochemical Tables*, 3rd ed.; American Chemical Society: Washington, DC, 1985; Vol. 14.

(16) Urdahl, R. S.; Bao, Y.; Jackson, W. M. An experimental determination of the heat of formation of C_2 and the C-H bond dissociation energy in C_2H. *Chem. Phys. Lett.* **1991**, *178* (4), 425−428.

(17) Dean, A. J.; Hanson, R. K.; Bowman, C. T. High temperature shock tube study of reactions of CH and C-atoms with N_2. *Twenty-Third Symposium (Int.) on Combustion*; The Combustion Institute, Pittsburgh, PA, 1990; Vol. 23, pp 259−265.

(18) Lindackers, D.; Burmeister, M.; Roth, P. Perturbation studies of high temperature C and CH reactions with N_2 and NO. *Twenty-Third Symposium (Int.) on Combustion*; The Combustion Institute, Pittsburgh, PA, 1990; Vol. 23, pp 251−257.

(19) Natarajan, K.; Woiki, D.; Roth, P. *Int. J. Chem. Kinet.*, in press.

(20) Slack, M. W.; Fishburne, E. S. Kinetics and Thermodynamics of the CN Molecule. I. Decomposition Mechanism for CN Molecules. *J. Chem. Phys.* **1970**, *52* (11), 5830−5833.

(21) Slack, M. W. Kinetics and Thermodynamics of the CN Molecule. III. Shock Tube Measurement of CN dissociation rates. *J. Chem. Phys.* **1976**, *64* (1), 228−236.

(22) Lutz, A. E.; Kee, R. J.; Miller, J. A. SENKIN: A FORTRAN Program for Predicting Homogeneous Gas Phase Chemical Kinetics with Sensitivity Analysis. SANDIA REPORT, SAND87-8248.UC-4; Sandia National Laboratories; Albuquerque, NM, 1988.